Eur. Phys. J. Plus (2013) **128**: 152
DOI 10.1140/epjp/i2013-13152-7

THE EUROPEAN PHYSICAL JOURNAL PLUS

Regular Article

Entropy-corrected holographic scalar field models of dark energy in Kaluza-Klein universe

M. Sharif[a] and Abdul Jawad[b]

Department of Mathematics, University of the Punjab, Quaid-e-Azam Campus, Lahore-54590, Pakistan

Received: 27 June 2013 / Revised: 13 September 2013
Published online: 10 December 2013 –

Abstract. We investigate the evolution of interacting holographic dark energy with logarithmic corrections in the flat Kaluza-Klein universe. We evaluate the equation of state parameter and also reconstruct the scalar field models in this scenario. For this purpose, the well-known choice of scale factor in the power law form is taken. It is interesting to mention here that the corresponding equation of state parameter crosses the phantom divide line for a particular choice of interacting parameters. Finally, we conclude that the behavior of the dynamical scalar field as well as the scalar potential is consistent with the present observations.

1 Introduction

The holographic dark energy (HDE) has attracted a lot of attention due to the global property of the universe (a direct relationship with spacetime). It is originated from quantum gravity and is based on the holographic principle proposed by Susskind [1]. Its mathematical formulation was given by Hsu [2] and Li [3] on the basis of the Cohen *et al.* relation [4]. This relation provides the bound on the vacuum energy Λ of a system with size L that should not cross the limit of the mass of a black hole having the same size due to the formation of a black hole in quantum field theory.

The interacting and non-interacting HDE models have been discussed extensively in general relativity [5–7] and also in its modified theories such as $f(R)$ [8], $f(R,T)$ [9], $f(T)$ [10], Brans-Dicke [11], Horava-Lifshitz [12], etc. Gong and Li [13] derived the HDE model in extra dimensions (called modified holographic dark energy (MHDE)) with the help of the $N+1$ dimensional mass of the Schwarzschild black hole [14]. The evolution of MHDE has been investigated by many people [13, 15] in the braneworld scenario and found interesting results. Recently, Sharif and his collaborators [16–18] have explored the MHDE from different aspects in the flat and non-flat Kaluza-Klein (KK) universe.

The definition of HDE was corrected through the entropy-corrected relation $S = A/4G + \tilde{\mu}\ln(A/4G) + \tilde{\lambda}$ in the scenario of loop quantum gravity [19]. Here A, G represent the area of horizon, gravitational constant, respectively, and $\tilde{\mu}$, $\tilde{\lambda}$ are physical constants of order of unity. This model is named as entropy-corrected HDE (ECHDE), while the exact values of constants involved in this model are still unknown. It was demonstrated that this type of DE model helps to explore the accelerated expansion of the universe. However, different phases of the universe can be characterized by an equation of state (EoS) parameter ω.

The reconstruction of scalar field DE models has been an interesting subject since last decade. These scalar field models deal with the dynamics of the scalar field and the corresponding potential. The motivation of the scalar field models occurs in particle physics as well as string theory [20] which help to explain the DE phenomenon. On the basis of different kinetic terms, these are characterized as quintessence, K-essence, tachyon and dilaton DE models etc. [20, 21]. Much of work has been done in the reconstruction of these models in the scenario of HDE [22–24] and ECHDE [25–27]. Recently, we have also established the correspondence of the HDE model (with Granda and Oliveros cutoff) with scalar field models in non-flat FRW [28] and flat KK [29] universes and found useful behavior of scalar field and corresponding potentials.

This paper is devoted to discussing the entropy-corrected version of HDE with event horizon in the flat KK universe. We also develop a correspondence of this model with scalar field DE models. The paper has the following

[a] e-mail: msharif.math@pu.edu.pk
[b] e-mail: jawadab181@yahoo.com

format: Section 2 contains the discussion of KK universe and evolution of ECHDE. In sect. 3, we construct the ECHDE version of dynamical scalar field DE models. Finally, we summarize our results in the last section.

2 Entropy-corrected holographic dark energy

In this section, we discuss the evolution of ECHDE interacting with dust-like dark matter (DM) in the context of compact KK universe whose metric is given by [16–18, 30–34]

$$\mathrm{d}s^2 = -\mathrm{d}t^2 + a^2(t)\left[\frac{\mathrm{d}r^2}{1-kr^2} + r^2(\mathrm{d}\theta^2 + \sin\theta^2\mathrm{d}\phi^2) + (1-kr^2)\mathrm{d}\psi^2\right], \tag{1}$$

where $a(t)$ indicates the cosmic scale factor and k represents the cosmic curvature which defines open, flat and closed KK universes accordingly $k = -1,\ 0,\ 1$. The generalized form of the field equations in $4+1$ dimensions is

$$R_{\mu\nu} - \frac{1}{2}g_{\mu\nu}R = \kappa T_{\mu\nu}, \quad (\mu,\ \nu = 0,1,2,3,4), \tag{2}$$

where $g_{\mu\nu}$, $R_{\mu\nu}$, R, $T_{\mu\nu}$ and κ are the metric tensor, the Ricci tensor, the Ricci scalar, the energy-momentum tensor and the coupling constant, respectively. We consider the flat KK universe with perfect fluid,

$$T_{\mu\nu} = (p+\rho)u_\mu u_\nu + p g_{\mu\nu}, \tag{3}$$

where $p = p_\Lambda$ represents pressure due to ECHDE, $\rho = \rho_\Lambda + \rho_m$ is the sum of energy densities due to ECHDE and DM and u_μ describes the five-velocity with $u^\mu u_\mu = -1$.

Kaluza had proposed an extra dimension to the fourth-dimensional theory of gravity in order to unify gravity and electromagnetism [35]. According to his viewpoint, there does not exist five-dimensional matter, the mathematical structure can be extended to five dimensions without any change and the quantities do not depend upon fifth coordinate. The last assumption is known as cylindrical condition and seems to be unnatural. However, the consequence of his work showed that the empty fifth dimension shows the presence of a 4-dimensional electromagnetic radiation and Maxwell's equations. Further developments on the Kaluza's work has been made by Klein. He proposed that extra dimension should be compact with a small diameter [36]. In other words, Klein proposed that the fifth dimension should be length, like a type of circle (*i.e.*, S^1 topology) having small radius. The circular topology implies periodicity as follows:

$$f(x,y) = f(\mathbf{x}, \mathbf{y} + 2\pi r_*), \qquad \mathbf{x} = (x^0, x^1, x^2, x^3), \qquad \mathbf{y} = x^4,$$

where r_* is the scale or radius of the fifth dimension.

Regarding the size of r_*, the strongest constraints come from high-energy particle physics which provides higher mass scales and corresponding smaller length scales. These experiments indicate that the length of r_* should be less than an attometer (1attometer $= 10^{-18}$) [37]. It is also argued that the fifth dimension seems to be a line at large distances, while close insights suggest small circles having radius less than the Planck length on the topology of R^4 geometry [38].

With the help of eqs. (2) and (3), one can obtain equations of motion for the non-flat KK universe as

$$H^2 + \frac{k}{a^2} = \frac{8\pi G}{6}\rho, \tag{4}$$

$$\dot{H} + 2H^2 + \frac{k}{a^2} = -\frac{8\pi G}{3}p, \tag{5}$$

where H appears as the Hubble parameter, dot represents differentiation with respect to cosmic time and we also assume $8\pi G = 1$. Also, ρ is the sum of energy densities of ECHDE and DM and p is the pressure only due to ECHDE. In this work, we consider only the flat case ($k = 0$) for which eq. (4) can be written in the form of fractional energy densities as

$$\Omega_m + \Omega_\Lambda = 1, \qquad \Omega_m = \frac{\rho_m}{6H^2}, \qquad \Omega_\Lambda = \frac{\rho_\Lambda}{6H^2}. \tag{6}$$

The corresponding non-conservation equations for DM and DE are

$$\dot{\rho}_m + 4H\rho_m = \Xi, \qquad \dot{\rho}_\Lambda + 4H(\rho_\Lambda + p_\Lambda) = -\Xi. \tag{7}$$

Here Ξ is an interaction term which can be taken as [39]

$$\Xi = 4d^2H(\rho_\Lambda - \rho_m),$$

and d^2 is a coupling constant. The ECHDE for KK universe takes the form [19]

$$\rho_\Lambda = 12m^2\pi^3 L^{-1} + \mu L^{-4}\ln(4\pi^3 L^3) + \lambda L^{-4}, \tag{8}$$

where m is constant and μ, λ are dimensionless constants of order of unity. For the flat universe, L is defined in terms of the future event horizon of the universe as [3]

$$L \equiv a(t)\int_a^\infty \frac{\mathrm{d}\tilde{a}}{H\tilde{a}^2} = a(t)\int_t^\infty \frac{\mathrm{d}\tilde{t}}{a(\tilde{t})}.$$

Also, the time derivative of L leads to

$$\dot{L} = HL - 1. \tag{9}$$

Making use of eqs. (6) and (8), we obtain

$$HL = \sqrt{\frac{12m^2\pi^3 L + \mu L^{-2}\ln(4\pi^3L^3) + \lambda L^{-2}}{6\Omega_\Lambda}}. \tag{10}$$

Consequently, eq. (9) becomes

$$\dot{L} = \sqrt{\frac{12m^2\pi^3 L + \mu L^{-2}\ln(4\pi^3L^3) + \lambda L^{-2}}{6\Omega_\Lambda}} - 1. \tag{11}$$

Differentiation of eq. (8) with respect to time yields

$$\begin{aligned}\dot{\rho}_\Lambda = &\left[3\mu L^{-5} - 12m^2\pi^3 L^{-2} - 4\mu L^{-5}\ln(4\pi^3L^3) - 4\lambda L^{-5}\right]\\ &\times\left[\left(12m^2\pi^3L + \mu L^{-2}\ln(4\pi^3L^3) + \lambda L^{-2}\right)^{\frac{1}{2}}(6\Omega_\Lambda)^{-\frac{1}{2}} - 1\right].\end{aligned} \tag{12}$$

Inserting the values of $\dot{\rho}_\Lambda$ and Ξ in eq. (7), we obtain

$$\begin{aligned}\omega_\Lambda = -1 - &\frac{3\mu L^{-4} - 12m^2\pi^3L^{-1} - 4\mu L^{-4}\ln(4\pi^3L^3) - 4\lambda L^{-4}}{4(12m^2\pi^3L^{-1} + \mu L^{-4}\ln(4\pi^3L^3) + \lambda L^{-4})}\\ &\times\left[1 - \sqrt{\frac{6\Omega_\Lambda}{12m^2\pi^3L + \mu L^{-2}\ln(4\pi^3L^3) + \lambda L^{-2}}}\right] - d^2\left(1 - \frac{\Omega_m}{\Omega_\Lambda}\right).\end{aligned} \tag{13}$$

This is the EoS parameter for the ECHDE which depends upon infrared (IR) cutoff parameter L. We would like to mention here that for the cosmological inflation in the early universe, the future event horizon and Hubble horizon coincide, *i.e.*, $L = H^{-1}$. In this case, eq. (13) takes the form

$$\begin{aligned}\omega_\Lambda = -1 - &\frac{3\mu H^4 - 12m^2\pi^3H - 4\mu H^4\ln(4\pi^3H^{-3}) - 4\lambda H^4}{4(12m^2\pi^3H + \mu H^4\ln(4\pi^3H^{-3}) + \lambda H^4)}\\ &\times\left[1 - \sqrt{\frac{6\Omega_\Lambda}{12m^2\pi^3H^{-1} + \mu H^2\ln(4\pi^3H^{-3}) + \lambda H^2}}\right] - d^2\left(1 - \frac{\Omega_m}{\Omega_\Lambda}\right).\end{aligned}$$

This is true only for the early inflation, radiation and matter-dominated phases of the universe. However, in our case, the correction terms play their role for the present status of the universe in which the total cosmic energy density is dominated by DE. For the present or later time, the future event horizon should be used as an IR cutoff.

To get insights of DE phases from eq. (13), we choose the scale factor of the form [40,41]

$$a(t) = a_0T^\alpha, \qquad T = \frac{t}{t_0}, \tag{14}$$

where a_0 represents the present value of the scale factor, α is the dimensionless positive parameter and t_0 is the present age of the universe. For constraining the model parameter α, various cosmological observations have already been made such as magnitude-redshift relation of supernovae type Ia [42,43], gravitational lensing statistics [44], the angular size redshift data of compact radio sources [45], the present age of the universe [46] and the primordial nucleosynthesis [47].

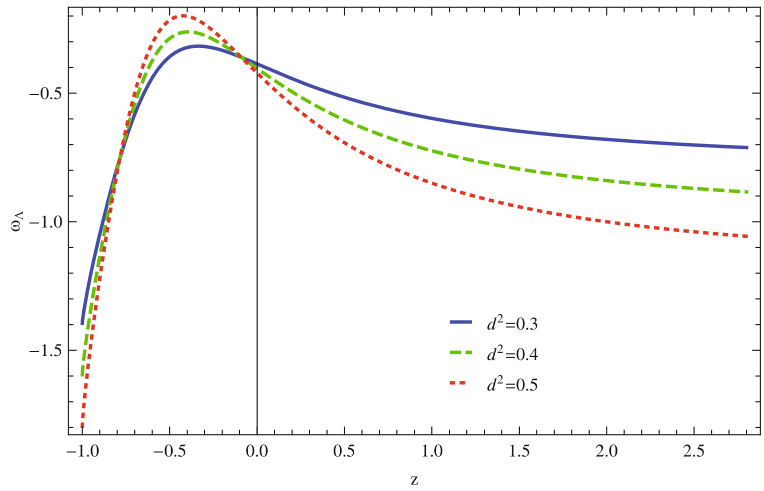

Fig. 1. Plot of ω_Λ *versus* z for ECHDE.

Recently, it is found that the power law of scale factor is compatible with the observational data about the accelerated expansion of the universe [40, 41].

In view of the above equation, the deceleration parameter q takes the form

$$q = \frac{1}{\alpha} - 1. \tag{15}$$

We note that $\alpha > 1$ or $\alpha < 1$ leads to $q < 0$ or $q > 0$, respectively, which describe the accelerating or decelerating nature of the universe. It is observed that the accelerated expansion of the universe can be obtained in the range $-1 < q < 0$.

In terms of deceleration parameter, the scale factor turns out to be

$$a(t) = a_0 T^{\frac{1}{1+q}}, \tag{16}$$

which implies

$$H = H_0(1+z)^{1+q}, \qquad L = -\frac{1}{qH_0}(1+z)^{-(1+q)}. \tag{17}$$

Here, we use the relation $a = a_0(1+z)^{-1}$, z is the redshift parameter and $H_0 = \frac{1}{t_0(1+q)}$ describes the present rate of expansion of the universe. Using eqs. (6), (8) and (17) in (13), it follows that

$$\begin{aligned}\omega_\Lambda = -1 - \frac{q+1}{4}&\left[\left(3\mu - 4\mu\ln\left(-\frac{4\pi^3}{q^3H_0^3}(1+z)^{-3(1+q)}\right) - 4\lambda\right)q^3H_0^3 - 12m^2\pi^3(1+z)^{-3(1+q)}\right]\\ &\times\left[\left(\mu\ln\left(-\frac{4\pi^3}{q^3H_0^3}(1+z)^{-3(1+q)}\right) + \lambda\right)q^3H_0^3 - 12m^2\pi^3(1+z)^{-3(1+q)}\right]^{-1}\\ &-d^2\left[2\left(\mu\ln\left(-\frac{4\pi^3}{q^3H_0^3}(1+z)^{-3(1+q)}\right) + \lambda\right)q^3H_0^3 - 24m^2\pi^3(1+z)^{-3(1+q)} - 6H_0q^{-1}(1+z)^{-2(1+q)}\right]\\ &\times\left[\left(\mu\ln\left(-\frac{4\pi^3}{q^3H_0^3}(1+z)^{-3(1+q)}\right) + \lambda\right)q^3H_0^3 - 12m^2\pi^3(1+z)^{-3(1+q)}\right]^{-1}.\end{aligned} \tag{18}$$

We plot this form of EoS parameter ω_Λ *versus* the redshift parameter z by taking different values of the interacting parameter $d^2 = 0.3,\ 0.4,\ 0.5$ as shown in fig. 1. Also, we assume $q = -0.18$ [40], $\mu = 0.005$, $\lambda = 0.5$, $m = 0.91$ [48] and $H_0 = 70$. The current value of EoS parameter for three cases of interacting parameter of this DE model is $\omega_{\Lambda_0} \simeq -0.4$. It is observed that ω_Λ evolutes the universe from quintessence region (at early, present and near future epoch) and goes towards phantom era (in the later time) which represents the phantom crossing for lower values of d^2, *i.e.*, 0.3, 0.4. The EoS parameter starts from phantom era for $z \geq 2.5$, remains in the quintessence region for $-0.8 < z < 2.5$ and then goes again to phantom era. However, EoS parameter evolves the ΛCDM model at $z = -0.8$ in all cases of interacting parameter.

3 Correspondence of ECHDE with scalar field dark energy models

In this section, we evaluate the scalar potential and dynamics of the scalar field models such as quintessence, tachyon, K-essence and dilation field (only scalar field) in the scenario of the interacting ECHDE.

3.1 Quintessence dark energy model

The quintessence scalar field models provide the scaling and attractor solutions which help to explain the phenomenon of accelerated expansion of the universe [21]. In terms of homogeneous and time-dependent scalar field ϕ, the energy density and pressure are defined as

$$\rho_\phi = \frac{1}{2}\dot{\phi}^2 + V(\phi), \qquad p_\phi = \frac{1}{2}\dot{\phi}^2 - V(\phi), \tag{19}$$

where $\dot{\phi}^2$ and $V(\phi)$ are called the kinetic energy and potential of the quintessence scalar field. In order to get the correspondence of this model with ECHDE, we equate $\rho_\phi = \rho_\Lambda$ and $p_\phi = p_\Lambda$. The corresponding EoS parameter turns out to be

$$\omega_\Lambda = \frac{\dot{\phi}^2 - 2V(\phi)}{\dot{\phi}^2 + 2V(\phi)}. \tag{20}$$

Also, eq. (19) leads to

$$\dot{\phi}^2 = (1+\omega_\Lambda)\rho_\Lambda, \qquad V(\phi) = \frac{1}{2}(1-\omega_\Lambda)\rho_\Lambda. \tag{21}$$

Inserting the values of ρ_Λ and ω_Λ from (8) and (18), respectively, in the above equation, we get

$$\begin{aligned}\dot{\phi}^2 = {} & \frac{q(q+1)H_0(1+z)^{4(1+q)}}{4}\left[\left(-3\mu + 4\mu\ln\left(-\frac{4\pi^3}{q^3H_0^3}(1+z)^{-3(1+q)}\right) + 4\lambda\right)q^3H_0^3 - 12m^2\pi^3(1+z)^{-3(1+q)}\right] \\ & + qd^2H_0(1+z)^{4(1+q)}\left[6H_0q^{-1}(1+z)^{-2(1+q)} - 2\left(\mu\ln\left(-\frac{4\pi^3}{q^3H_0^3}(1+z)^{-3(1+q)}\right) + \lambda\right)q^3H_0^3\right. \\ & \left. + 24m^2\pi^3(1+z)^{-3(1+q)}\right],\end{aligned} \tag{22}$$

$$\begin{aligned}V(\phi) = {} & \frac{q(q+1)H_0(1+z)^{4(1+q)}}{8}\left[\left(3\mu - 4\mu\ln\left(-\frac{4\pi^3}{q^3H_0^3}(1+z)^{-3(1+q)}\right) + 4\lambda\right)q^3H_0^3 + 12m^2\pi^3(1+z)^{-3(1+q)}\right] \\ & + qH_0(1+d^2)(1+z)^{4(1+q)} \times \left[\left(\mu\ln\left(-\frac{4\pi^3}{q^3H_0^3}(1+z)^{-3(1+q)}\right) + \lambda\right)q^3H_0^3 - 12m^2\pi^3(1+z)^{-3(1+q)}\right] \\ & - 3d^2H_0^2(1+z)^{2(1+q)}.\end{aligned} \tag{23}$$

We can find the scalar field ϕ from (22) as

$$\begin{aligned}\phi(z) = {} & \int_0^z \left[\frac{q(q+1)H_0(1+z)^{4(1+q)}}{4}\left[\left(4\mu\ln\left(-\frac{4\pi^3}{q^3H_0^3}(1+z)^{-3(1+q)}\right) - 3\mu + 4\lambda\right)q^3H_0^3 - 12m^2\pi^3(1+z)^{-3(1+q)}\right]\right. \\ & + d^2H_0(1+z)^{4(1+q)}\left[6H_0(1+z)^{-2(1+q)} - 2\left(\mu\ln\left(-\frac{4\pi^3}{q^3H_0^3}(1+z)^{-3(1+q)}\right) + \lambda\right)q^3H_0^3\right. \\ & \left.\left. - 24m^2\pi^3(1+z)^{-3(1+q)}\right]\right]^{\frac{1}{2}} \frac{1}{H_0(1+z)^{2+q}}\mathrm{d}z.\end{aligned} \tag{24}$$

We solve this equation numerically in terms of z and plot it by assuming the same parameters as mentioned in previous section. This is shown in fig. 2 indicating that the quintessence scalar field shows decreasing behavior with respect to z. Figure 3 shows that the scalar potential also decreases with the increase of interacting parameter d^2 with respect to z. Also, the scalar potential $V(\phi)$ increases with the scalar field $\phi(z)$ and becomes more steeper for larger values of d^2 as shown in fig. 4.

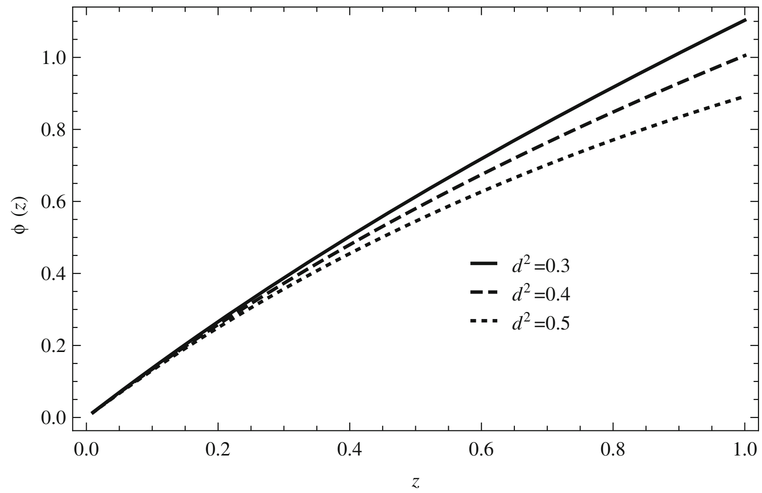

Fig. 2. Plot of ϕ *versus* z for the quintessence model.

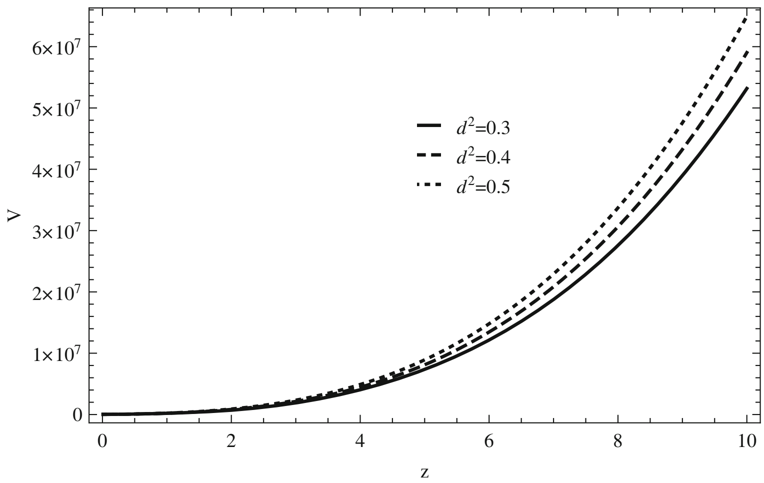

Fig. 3. Plot of V *versus* z for the quintessence model.

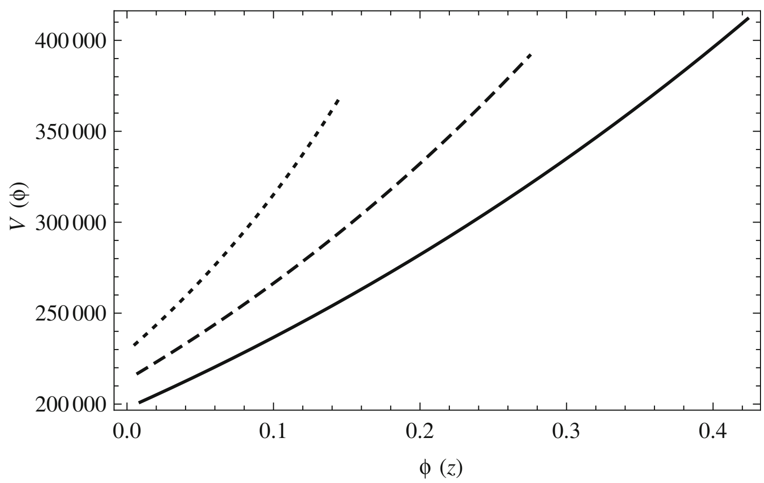

Fig. 4. Plot of $V(\phi)$ *versus* $\phi(z)$ for the quintessence model.

3.2 Tachyon dark energy model

It was argued [49] that the accelerated expansion of the universe takes place under the rolling down of the tachyon field. After that a particular epoch will occur when the scale factor crosses the point of inflection marking at the end of inflation. The rolling tachyon has an interesting feature to evolute the EoS parameter between −1 and 0 [50], which is used as a useful candidate at high energy. A large number of attempts have been made to construct the reliable cosmological models by giving variation to tachyon potentials [51–53]. The energy and pressure of the tachyon DE model has the form

$$\rho_t = \frac{V(\phi)}{\sqrt{1-\dot{\phi}^2}}\,,$$
$$p_t = -V(\phi)\sqrt{1-\dot{\phi}^2}. \tag{25}$$

The corresponding EoS parameter becomes

$$\omega_t = \dot{\phi}^2 - 1. \tag{26}$$

We assume $\rho_t = \rho_\Lambda$ and $p_t = p_\Lambda$ in order to get the correspondence between ECHDE and tachyon model which give rise to

$$\begin{aligned}\dot{\phi}^2 = &-\frac{q+1}{4}\left[\left(3\mu - 4\mu\ln\left(-\frac{4\pi^3}{q^3H_0^3}(1+z)^{-3(1+q)}\right) - 4\lambda\right)q^3H_0^3 - 12m^2\pi^3(1+z)^{-3(1+q)}\right]\\
&\times\left[\left(\mu\ln\left(-\frac{4\pi^3}{q^3H_0^3}(1+z)^{-3(1+q)}\right)+\lambda\right)q^3H_0^3 - 12m^2\pi^3(1+z)^{-3(1+q)}\right]^{-1}\\
&- d^2\left[2\left(\mu\ln\left(-\frac{4\pi^3}{q^3H_0^3}(1+z)^{-3(1+q)}\right)+\lambda\right)q^3H_0^3\right.\\
&\left.- 24m^2\pi^3(1+z)^{-3(1+q)} - 6H_0q^{-1}(1+z)^{-2(1+q)}\right]\\
&\times\left[\left(\mu\ln\left(-\frac{4\pi^3}{q^3H_0^3}(1+z)^{-3(1+q)}\right)+\lambda\right)q^3H_0^3 - 12m^2\pi^3(1+z)^{-3(1+q)}\right]^{-1},\end{aligned} \tag{27}$$

$$\begin{aligned}V(\phi) = qH_0(1+z)^{4(1+q)}&\left[-1-\frac{q+1}{4}\left[\left(3\mu - 4\mu\ln\left(-\frac{4\pi^3}{q^3H_0^3}(1+z)^{-3(1+q)}\right) - 4\lambda\right)q^3H_0^3\right.\right.\\
&\left.- 12m^2\pi^3(1+z)^{-3(1+q)}\right]\left[\left(\mu\ln\left(-\frac{4\pi^3}{q^3H_0^3}(1+z)^{-3(1+q)}\right)+\lambda\right)q^3H_0^3\right.\\
&\left.- 12m^2\pi^3(1+z)^{-3(1+q)}\right]^{-1} - d^2\left[2q^3H_0^3\left(\mu\ln\left(-\frac{4\pi^3}{q^3H_0^3}(1+z)^{-3(1+q)}\right)+\lambda\right)\right.\\
&\left.- 24m^2\pi^3(1+z)^{-3(1+q)} - (1+z)^{-2(1+q)}6H_0q^{-1}\right]\\
&\left.\times\left[\left(\mu\ln\left(-\frac{4\pi^3}{q^3H_0^3}(1+z)^{-3(1+q)}\right)+\lambda\right)q^3H_0^3 - 12m^2\pi^3(1+z)^{-3(1+q)}\right]^{-1}\right]^{\frac{1}{2}}\\
&\times\left[\left(\mu\ln\left(-\frac{4\pi^3}{q^3H_0^3}(1+z)^{-3(1+q)}\right)+\lambda\right)q^3H_0^3 - 12m^2\pi^3(1+z)^{-3(1+q)}\right].\end{aligned} \tag{28}$$

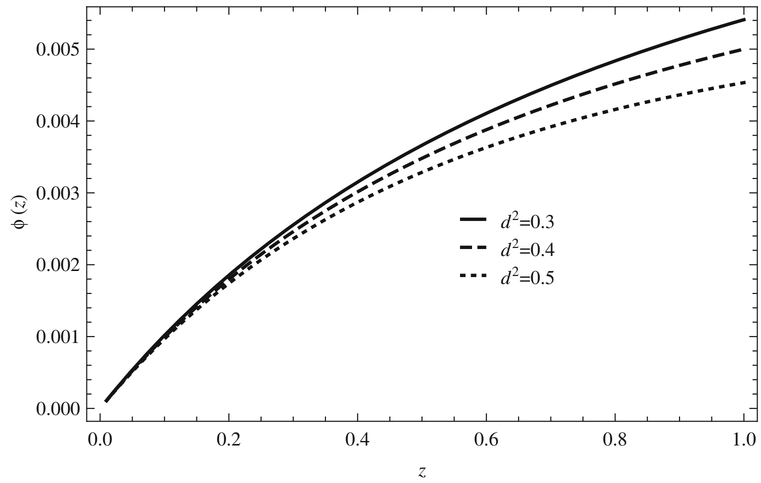

Fig. 5. Plot of ϕ *versus* z for the tachyon model.

From eq. (27), we obtain the tachyon scalar field,

$$\phi(z) = \int_0^z \frac{(1+z)^{-(1+q)}}{H_0}\left[\frac{q+1}{4}\left[\left(-3\mu+4\mu\ln\left(-\frac{4\pi^3}{q^3H_0^3}(1+z)^{-3(1+q)}\right)-4\lambda\right)q^3H_0^3+12m^2\pi^3(1+z)^{-3(1+q)}\right]\right.$$
$$\times\left[\left(\mu\ln\left(-\frac{4\pi^3}{q^3H_0^3}(1+z)^{-3(1+q)}\right)+\lambda\right)q^3H_0^3-12m^2\pi^3(1+z)^{-3(1+q)}\right]^{-1}$$
$$-\,\mathrm{d}^2\left[2q^3H_0^3\left(\mu\ln\left(-\frac{4\pi^3}{q^3H_0^3}(1+z)^{-3(1+q)}\right)+\lambda\right)-24m^2\pi^3(1+z)^{-3(1+q)}6H_0q^{-1}(1+z)^{-2(1+q)}\right]$$
$$\left.\times\left[\left(\mu\ln\left(-\frac{4\pi^3}{q^3H_0^3}(1+z)^{-3(1+q)}\right)+\lambda\right)q^3H_0^3 12m^2\pi^3(1+z)^{-3(1+q)}\right]^{-1}\right]^{\frac{1}{2}}. \tag{29}$$

The analytical form of the tachyon scalar field $\phi(z)$ cannot be obtained but we can solve it numerically as shown in fig. 5. Notice that it increases initially but becomes flat and attains a minimum finite value (with the increase of d^2) at high redshift. This shows that the tachyon scalar field decreases with the expansion of the universe. We also plot the tachyon potential $V(\phi)$ *versus* z as shown in fig. 6 which attains a very large value at high redshift. Similar to quintessence case, fig. 7 shows that the tachyon potential *versus* tachyon field $\phi(z)$ becomes more steeper for large value of interacting parameter d^2. It is remarked that the tachyon field rolls down the potential slowly with the expansion of the universe.

3.3 K-essence dark energy model

This is another model to explain the accelerated expansion of the universe. It was originated through the modification of kinetic energy of the scalar field models. Initially, it was used by Armendáriz-Picón *et al.* [54,55] to discuss the early inflation at high energies. Chiba *et al.* [56] turned this scenario towards the DE phenomenon. Later, it was generalized by Armendáriz-Picón *et al.* [57,58]. The energy density and pressure for the K-essence model are

$$\rho_k = V(\phi)(-\chi+3\chi^2),$$
$$p_k = V(\phi)(-\chi+\chi^2), \tag{30}$$

where $\chi = \frac{1}{2}\dot{\phi}^2$ and $V(\phi)$ denotes the scalar potential of the K-essence model. The corresponding EoS parameter is

$$\omega_k = \frac{1-\chi}{1-3\chi}, \tag{31}$$

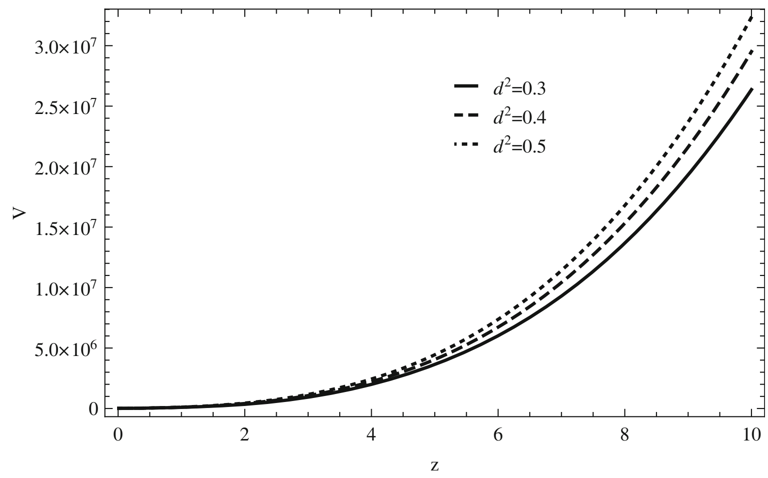

Fig. 6. Plot of V *versus* z for the tachyon model.

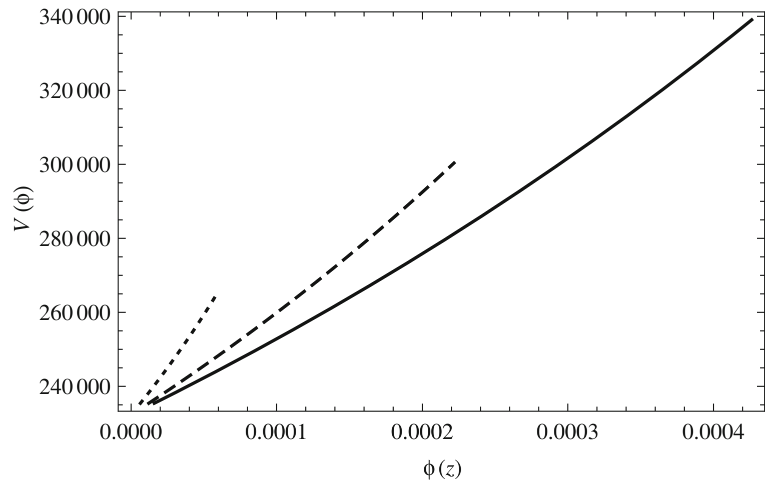

Fig. 7. Plot of $V(\phi)$ *versus* $\phi(z)$ for the tachyon model.

which shows that the accelerated expansion can be achieved for $\chi \in (\frac{1}{3}, \frac{2}{3})$. By setting $\rho_k = \rho_\Lambda$ and $p_k = p_\Lambda$, we obtain

$$\chi = \frac{\omega_\Lambda - 1}{3\omega_\Lambda - 1}, \tag{32}$$

$$V(\phi) = \frac{(1-3\omega_\Lambda)^2 q H_0 (1+z)^{4(1+q)}}{1-\omega_\Lambda} \times \left[\left(\mu \ln\left(-\frac{4\pi^3}{q^3 H_0^3}(1+z)^{-3(1+q)}\right) + \lambda\right) q^3 H_0^3 - 12 m^2 \pi^3 (1+z)^{-3(1+q)}\right]. \tag{33}$$

The graph of χ *versus* z in fig. 8 shows the accelerated expansion of the universe exactly lying in the required interval with the same assumptions of constant parameters as in the previous section. Also, this shows that the kinetic energy of the model decreases more rapidly with the increment of interacting parameter. The expression $\chi = \frac{1}{2}\dot{\phi}^2$ implies

$$\phi(z) = \int_0^z \frac{1}{H_0(1+z)^{2+q}} \sqrt{\frac{\omega_\Lambda - 1}{2(3\omega_\Lambda - 1)}} \mathrm{d}z. \tag{34}$$

Its graphical behavior is shown in fig. 9, which represents the increasing behavior and becomes finite at high redshift. Also, the potential starts from very high value and goes towards the positive minima obeying the inverse square law expansion shown in fig. 10.

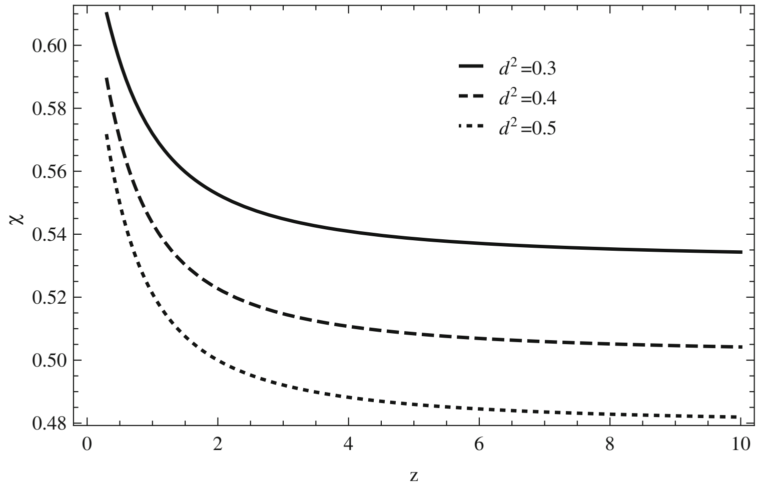

Fig. 8. Plot of χ *versus* z for the K-essence model.

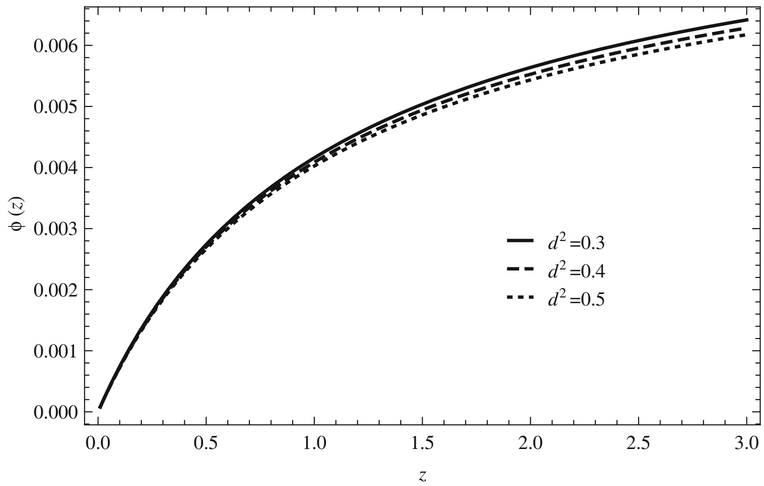

Fig. 9. Plot of $\phi(z)$ *versus* z for the K-essence model.

3.4 Dilaton dark energy model

The dilaton field is used as an alternative candidate to explain the DE puzzle. Its pressure and energy density are [20]

$$p_d = -\chi + b_1 e^{b_2\phi}\chi^2, \qquad \rho_d = -\chi + 3b_1 e^{b_2\phi}\chi^2, \tag{35}$$

where b_1 and b_2 are positive constants. The EoS for dilaton DE is

$$\omega_d = \frac{-1 + b_1 e^{b_2\phi}\chi}{-1 + 3b_1\ e^{b_2\phi}\chi}\,. \tag{36}$$

For correspondence, we equate $\rho_d = \rho_\Lambda$ and $p_d = p_\Lambda$, which give

$$e^{b_2\phi}\chi = \frac{\omega_\Lambda - 1}{b_1(3\omega_\Lambda - 1)}\,. \tag{37}$$

Here we observe that the EoS parameter (36) provides the range $(\frac{20}{63}, \frac{40}{63})$ for $e^{b_2\phi}\chi$ in order to obtain the accelerated universe. Figure 11 shows that $e^{b_2\phi}\chi$ lies exactly in this interval with $b_1 = 1.05$ (keeping the remaining constant parameters same) which provides the consistency of the results. Finally, the solution of (37) has the following form:

$$\phi(z) = \frac{2}{b_2}\ln\left[1 + \frac{b_2}{2}\int_0^z \frac{1}{H_0 1 + z)^{2+q}}\sqrt{\frac{\omega_\Lambda - 1}{2b_1(3\omega_\Lambda - 1)}}\mathrm{d}z\right]. \tag{38}$$

Its plot with respect to z is given in fig. 12 with $b_2 = 1.05$ which exhibits the similar behavior as the K-essence scalar field.

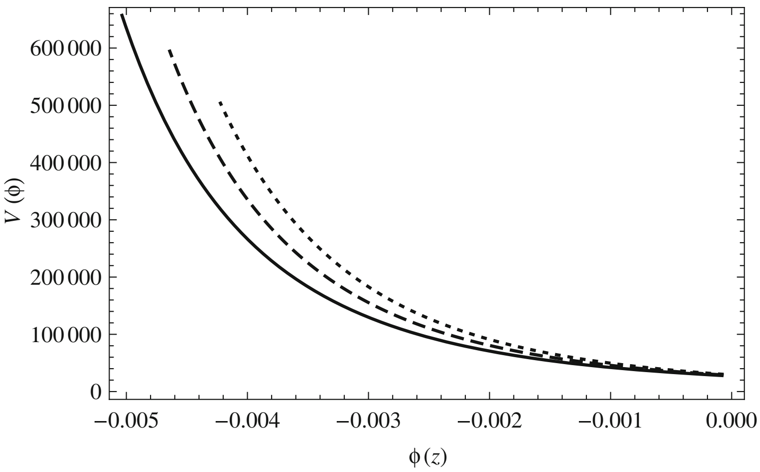

Fig. 10. Plot of $V(\phi)$ *versus* ϕ for the K-essence model.

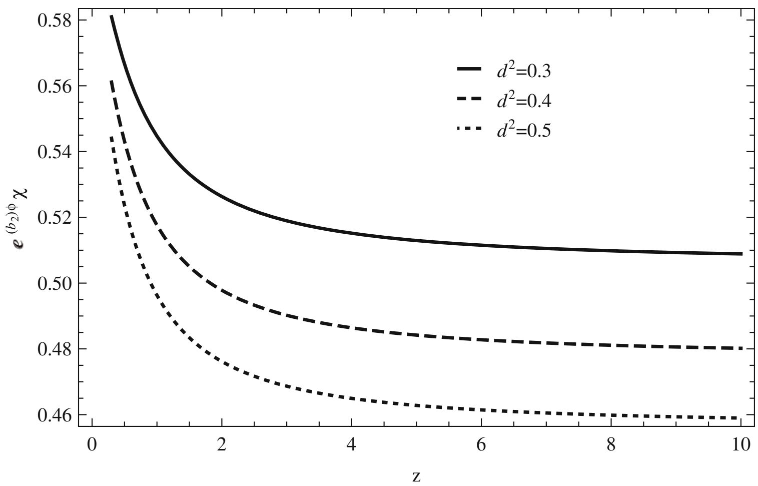

Fig. 11. Plot of $e^{b_2\phi}\chi$ *versus* z for the dilaton field.

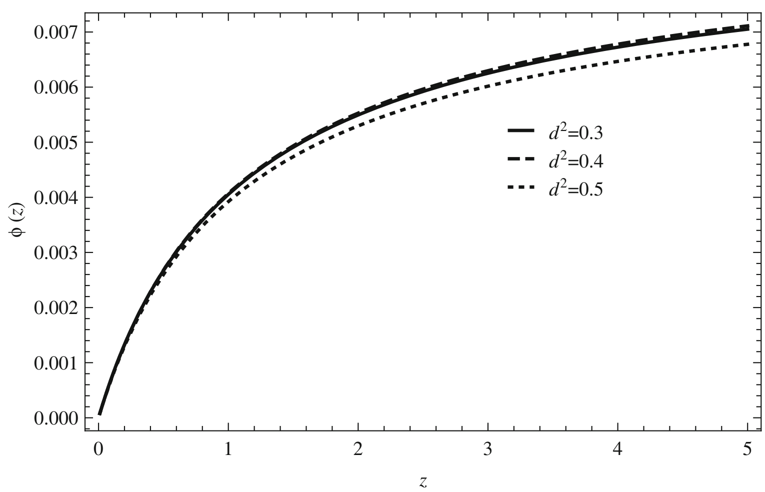

Fig. 12. Plot of ϕ *versus* z for the dilaton field.

4 Summary

The purpose of this paper is twofold: Firstly we have demonstrated the evolution of the universe by considering interacting ECHDE in the flat KK universe. To this end, we consider the well-known power law for scale factor consistent with the present observations [40]. The interacting parameter d^2 plays an important role in the graphical description of the results. We have seen that the smaller values of interacting parameter, *i.e.*, $d^2 = 0.3,\ 0.4$ have kept the EoS parameter of ECHDE in quintessence DE era at early, present and near future epoch while leads to phantom era at $z > -0.8$. For the third interacting case, the EoS parameter remains in the phantom phase for the ranges $z \geq 2.5$ and $z < -0.8$ and in the quintessence era for the range $-0.8 < z < 2.5$. We have also pointed out that the EoS parameter corresponds to ΛCDM model for $z = -0.8$ for all cases of interacting parameter. The result is shown in fig. 1.

It is pointed out that the selected choices of parameters can provide phantom crossing behavior of EoS parameter for interacting ECHDE with event horizon cutoff in the context of general relativity [25]. Besides the phantom energy, another important implication of ECHDE is that it can explain the cosmological inflation in the early universe. In our case, the EoS parameter also provides phantom crossing and explains the early inflation era of the universe. For interacting ECHDE (with Granda-Oliveros cutoff) in the context of general relativity, it is suggested that the EoS parameter (at Ricci scale) approaches to $-\frac{1}{3}$ when cosmic time approaches to infinity [59]. Also, it is argued that ECHDE with Ricci scalar cutoff may provide phantom crossing in the limiting case [60]. In our case, the value of EoS parameter approaches to $-1.4,\ -1.6,\ -1.8$ for $d^2 = 0.3,\ 0.4,\ 0.5$, respectively, when z approaches -1 and provides phantom crossing as well. Hence our result of EoS parameter is consistent with the suggested behavior of ECHDE in general relativity [25, 60].

By using different combination of observational schemes, Ade *et al.* [61] have put the following constraints on the EoS parameter:

$$\begin{aligned}
\omega_\Lambda &= -1.13^{+0.24}_{-0.25} && \text{(Planck+WP+BAO)},\\
\omega_\Lambda &= -1.09 \pm 0.17 && \text{(Planck+WP+Union 2.1)},\\
\omega_\Lambda &= -1.13^{+0.13}_{-0.14} && \text{(Planck+WP+SNLS)},\\
\omega_\Lambda &= -1.24^{+0.18}_{-0.19} && \text{(Planck+WP+}H_0\text{)},
\end{aligned}$$

at 95% confidence level. It can be seen from fig. 1 that the EoS parameter also meets the above-mentioned values for all cases of the interacting parameter which shows consistency with our results.

Secondly, we have established the correspondence of interacting ECHDE with the scalar field models. For this purpose, we have investigated the dynamics of scalar field and the corresponding scalar potential for quintessence, tachyon, K-essence and dilaton scalar field DE models as shown in figs. 2–12. It is worthwhile to mention here that the dynamics of the scalar field shows consistency in all scalar field models and attains finite value for high redshift. This indicates that the scalar field decreases with the accelerated universe. Moreover, the potential energy of the quintessence and tachyon models increases, while the K-essence potential energy goes towards positive minima. Finally, we would like to mention here that our results of dynamics of scalar field and potential for interacting ECHDE with power law ansatz are consistent with the results of Zhang [62] for quintessence HDE, for tachyon HDE [63–65] and Rozas-Fernández [66] for dilaton HDE models.

References

1. L. Susskind, J. Math. Phys. **36**, 6377 (1995).
2. S.D.H. Hsu, Phys. Lett. B **594**, 13 (2004).
3. M. Li, Phys. Lett. B **603**, 1 (2004).
4. A. Cohen, D. Kaplan, A. Nelson, Phys. Rev. Lett. **82**, 4971 (1999).
5. Q.G. Huang, M. Li, JCAP **04**, 013 (2004).
6. M. Jamil, E.N. Saridakis, M.R. Setare, Phys. Lett. B **679**, 172 (2009).
7. J. Lu *et al.*, JCAP **03**, 031 (2010).
8. K. Karami, M.S. Khaledian, JHEP **03**, 86 (2011).
9. M.J.S. Houndjo, O.F. Piattella, Int. J. Mod. Phys. D **2**, 1250024 (2012).
10. M.H. Daouda, M.E. Rodrigues, M.J.S. Houndjo, Eur. Phys. J. C **72**, 1893 (2012).
11. M.R. Setare, M. Jamil, Phys. Lett. B **690**, 1 (2010).
12. M.R. Setare, M. Jamil, JCAP **02**, 010 (2010).
13. Y. Gong, T. Li, Phys. Lett. B **683**, 241 (2010).
14. R.C. Myers, Phys. Rev. D **35**, 455 (1987).
15. D.J. Liu, H. Wang, B. Yang, Phys. Lett. B **694**, 6 (2010).

16. M. Sharif, F. Khanum, Gen. Relativ. Gravit. **43**, 2885 (2011).
17. M. Sharif, A. Jawad, Astrophys. Space Sci. **337**, 789 (2012).
18. M. Sharif, A. Jawad, Eur. Phys. J. C **72**, 1901 (2012).
19. H. Wei, Commun. Theor. Phys. **52**, 743 (2009).
20. F. Piazza, S. Tsujikawa, JCAP **07**, 004 (2004).
21. E.J. Copeland, M. Sami, S. Tsujikawa, Int. J. Mod. Phys. D **15**, 1753 (2006).
22. L. Granda, A. Oliveros, Phys. Lett. B **671**, 199 (2009).
23. K. Karami, J. Fehri, Phys. Lett. B **684**, 61 (2010).
24. A. Sheykhi, Phys. Rev. D **84**, 107302 (2011).
25. M. Jamil, M.U. Farooq, JCAP **03**, 001 (2010).
26. M.U. Farooq, M.A. Rashid, M. Jamil, Int. J. Theor. Phys. **49**, 2278 (2010).
27. K. Karami, M.S. Khaledian, M. Jamil, Phys. Scr. **83**, 025901 (2011).
28. M. Sharif, A. Jawad, Eur. Phys. J. C **72**, 2097 (2012).
29. M. Sharif, A. Jawad, Commun. Theor. Phys. **60**, 183 (2013).
30. G.S. Khadekar, V. Patki, Int. J. Theor. Phys. **47**, 1751 (2008).
31. G.S. Khadekar, R. Wanjari, C. Ozel, Int. J. Theor. Phys. **48**, 2550 (2009).
32. G.S. Khadekar, V. Kamdi, Int. J. Theor. Phys. **48**, 3147 (2009).
33. C. Ozel, H. Kayhan, G.S. Khadekar, Ad. Studies. Theor. Phys. **4**, 117 (2010).
34. M.I. Wanas, G.G.L. Nashed, A.A. Nowaya, Chin. Phys. B **21**, 049801 (2012).
35. T. Kaluza, Sitz. Press. Akad. Wiss. Phys. Math. **k1**, 966 (1921).
36. O. Klein, Z. Phys. **37**, 895 (1926).
37. V.A. Kostelecky, S. Samuel, Phys. Lett. B **270**, 21 (1991).
38. J.M. Overduin, P.S. Wesson, Phys. Rep. **283**, 303 (1997).
39. C.Y. Sun, R.H. Yue, Phys. Rev. D **85**, 043010 (2012).
40. S. Kumar, Mon. Not. R. Astron. Soc. **422**, 2532 (2012).
41. Z.H. Zhu *et al.*, Astron. Astrophys. **483**, 15 (2008).
42. A. Dev, M. Sethi, D. Lohiya, Phys. Lett. B **504**, 207 (2001).
43. G. Sethi, A. Dev, D. Jain, Phys. Lett. B **624**, 135 (2005).
44. A. Dev *et al.*, Phys. Lett. B **548**, 12 (2002).
45. D. Jain, A. Dev, J.S. Alcaniz, Class. Quantum Grav. **20**, 4163 (2003).
46. M. Kaplinghat *et al.*, Phys. Rev. D **59**, 043514 (1999).
47. M. Kaplinghat, G. Steigman, T.P. Walker, Phys. Rev. D **61**, 103507 (2000).
48. X. Zhang, F.Q. Wu, Phys. Rev. D **72**, 043524 (2005).
49. M. Sami, P. Chingangbam, T. Qureshi, Phys. Rev. D **66**, 043530 (2002).
50. G.W. Gibbons, Phys. Lett. B **537**, 1 (2002).
51. A. Mazumdar, S. Panda, A. Perez-Lorenzana, Nucl. Phys. B **614**, 101 (2001).
52. A. Feinstein, Phys. Rev. D **66**, 063511 (2002).
53. Y.S. Piao *et al.*, Phys. Rev. D **66**, 121301 (2002).
54. C. Armendáriz-Picón, T. Damour, V. Mukhanov, Phys. Lett. B **458**, 209 (1999).
55. J. Garriga, V. Mukhanov, Phys. Lett. B **458**, 2019 (1999).
56. T. Chiba, T. Okabe, M. Yamaguchi, Phys. Rev. D **62**, 023511 (2000).
57. C. Armendáriz-Picón, V. Mukhanov, P.J. Steinhardt, Phys. Rev. Lett. **85**, 4438 (2000).
58. C. Armendáriz-Picón, V. Mukhanov, P.J. Steinhardt, Phys. Rev. D **63**, 103510 (2001).
59. A. hodam-Mohammadi *et al.*, Astrophys. Space Sci. **345**, 415 (2013).
60. A. Pasqua *et al.*, Astrophys. Space Sci. **340**, 199 (2012).
61. P.A.R Ade *et al.*, arXiv:1303.5076.
62. X. Zhang, Phys. Lett. B **648**, 1 (2007).
63. J. Zhang, X. Zhang, X.H. Liu, Phys. Lett. B **651**, 84 (2007).
64. M.R. Setare, Phys. Lett. B **653**, 116 (2007).
65. A. Rozas-Fernández, D. Brizuela, N. Cruz, Int. J. Mod. Phys. D **19**, 573 (2010).
66. A. Rozas-Fernández, Eur. Phys. J. C **71**, 1536 (2011).